



Epimetheus Engine Development

PRELIMINARY DESIGN REVIEW

10/13/2025



SOCIETY OF AERONAUTICS AND ROCKETRY

Cesar Briones, Ramy Ismail

Table of Content

1 Introduction.....	2
1.1 Project Overview.....	2
1.2 Key Performance Parameters.....	3
2 Requirements.....	3
3 Injector.....	4
3.1 Design Overview.....	4
3.2 Fuel Element.....	5
3.3 Oxidizer Element.....	5
3.4 O-rings.....	6
3.5 Flow Simulation.....	6
3.6 Single Element Assembly.....	8
3.7 Georgia Tech Heritage.....	8
4 Feed System.....	9
5 Igniter.....	10
6 Engine Walls.....	10
6.1 Combustion Chamber.....	10
6.2 Nozzle.....	11
7 Burn time and Cooling Methods.....	12
8 Test stand Integration.....	14
9 Manufacturing.....	14

Table of Tables

Table 1. Expected Performance.....	4
Table 2. Combustion Properties.....	4
Table 3. Propellant Information.....	4
Table 4. Injector Properties.....	5
Table 5. Combustion Chamber dimensions.....	11
Table 6. Nozzle dimensions.....	12

Table of Figures

Figure 1. Epimetheus CAD Assembly.....	2
Figure 2. Injector CAD Assembly.....	4
Figure 3. Fuel Element CAD.....	5
Figure 4. Oxidizer Element CAD.....	5
Figure 5. Single Element CFD VOF Simulation.....	7
Figure 6. Injector Assembly CFD Mixture Simulation.....	7
Figure 7. Single Element Assembly.....	8
Figure 8. Georgia Tech Single Element water flow test.....	8
Figure 9. Chamber Wall CAD.....	10



Figure 10. Nozzle CAD.....	11
Figure 11. Heat Flux along the engine at different wall temperatures.....	12
Figure 12. SolidWorks Thermal FEA at 10 seconds.....	13
Figure 13. SolidWorks Thermal FEA chamber and nozzle nodes.....	13
Figure 14. Temperatures over time of chosen nodes.....	14



1 Introduction

1.1 Project Overview

This engine was developed with the objective to learn more about liquid propulsion. It started as a summer theoretical project, but after several design iterations, the team is looking forward to making this engine a reality.

Given that the purpose of this engine is to deepen the team's understanding of liquid propulsion, this engine was designed without flying considerations. Its project cycle will be complete and retired after a successful hot fire test. The team is dedicated to document the development and testing of this engine for not only the team's sake but also future generations. The full CAD assembly of the engine is shown below.

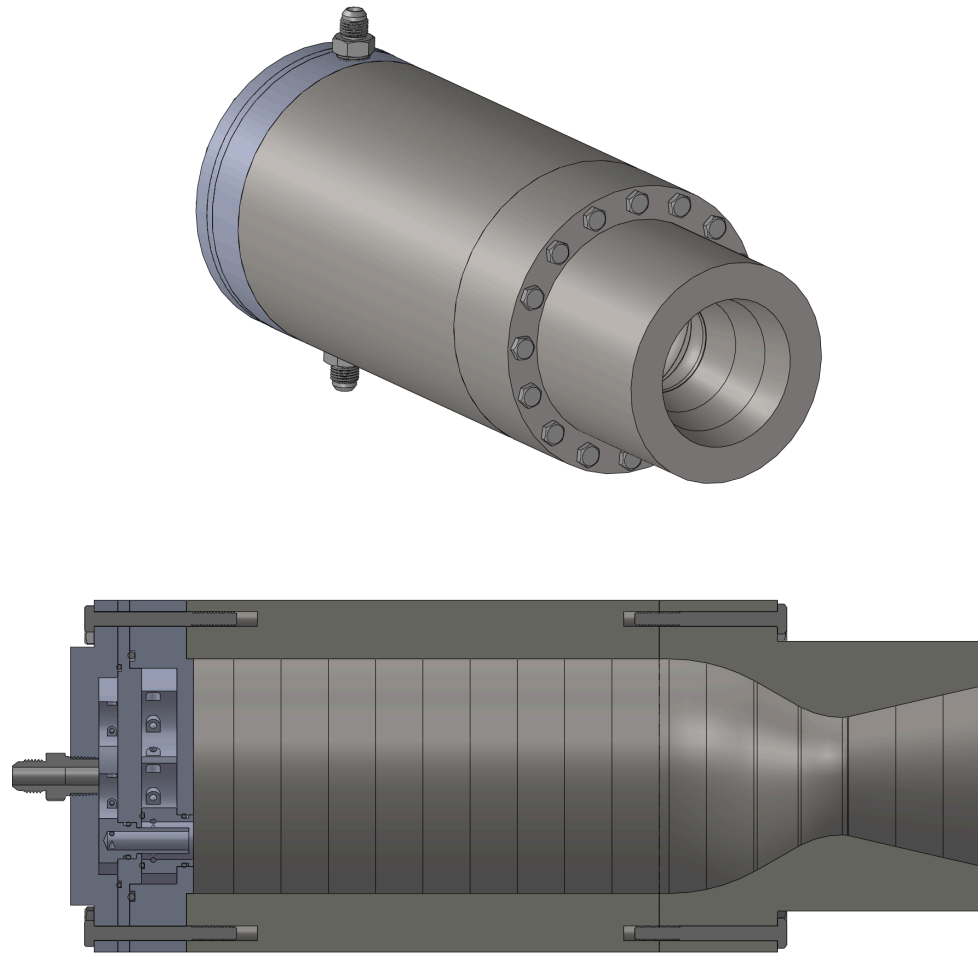


Figure 1. Epimetheus CAD Assembly



1.2 Key Performance Parameters

The engine was designed not with the intent to be perfectly optimized. Key design characteristics are shown below.

Table 1. Expected Performance

Parameter	Value	units
Characteristic Velocity	1485	m/s
Effective Exhaust Velocity	1814	m/s
Specific Impulse	185	s
Thrust Coefficient	1.22	(unitless)
Thrust	2.37	kN

Table 2. Combustion Properties

Combustion Properties	Injector	Nozzle Throat	Nozzle Exit	units
Pressure	1	0.565	0.1103	MPA
Temperature	2943	2757	2123	K
Density	1.03	0.6285	0.1482	kg/m ³
Mach Number	0	1	2.12	(unitless)

Table 3. Propellant Information

Propellant	Mass Flowrate (kg/s)
N2O	1.054
C2H5OH 95%	0.251

Table 4. Other Information

Property	Value	units
OF ratio	4.2	-
Burn Time	6	s



2 Requirements

The team recognizes the importance of well-defined requirements in guiding the development process. These requirements were carefully selected to provide clear boundaries for the engine's design, ensuring that performance, safety, and reliability objectives are met.

Table 5. Requirement Table

Req. ID	Requirement	Rationale
Req. 1	The engine shall hit at least 2000 N of thrust	Setting a goal for the engine design
Req. 2	The engine shall use Nitrous Oxide and Ethanol	Constrain the propellant choices
Req. 3	The engine shall use a heat sink as a thermal mitigation method	Constrain the thermal mitigation methods
Req. 4	The engine shall be able to be integrated into the current test stand	Critical for testing
Req. 5	The engine shall burn for at least 3 seconds	Constrain for burn time

[Page left blank on purpose]



3 Injector

3.1 Design Overview

The injector type chosen for this engine is the coaxial swirl injector type. It combines the fuel and oxidizer by leveraging the high tangential momentum at the exit of the injector. Small orifices inlets are placed at the start of a tube, where the propellant is pressurized. This specific configuration uses tip mixing so the fuel mixes with the oxidizer at the tip, right before leaving the injector.

The injector was designed following MATLAB and equations from “Experimental and Theoretical Study on Spray Angles of Bi-Swirl Coaxial Injectors” by W. Yoon and K. Ahn. Injector Assembly and properties are shown below.

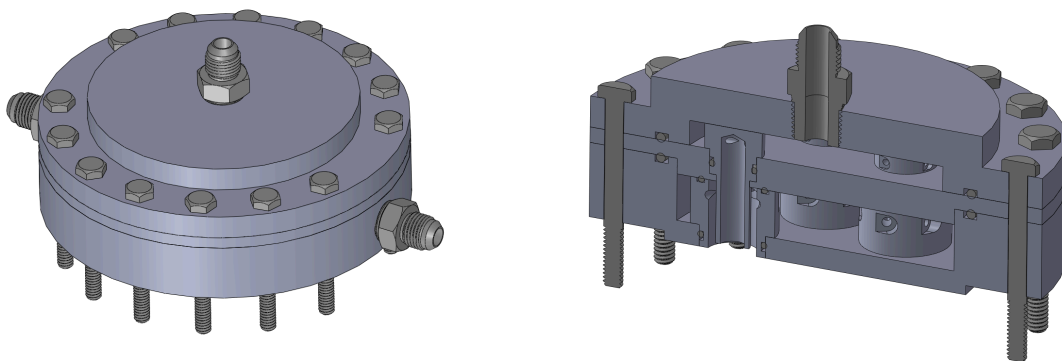


Figure 2. Injector CAD Assembly

Table 6. Injector Properties

Parameter	Inner (Fuel)	Outer (Oxidizer)	Tip-Mix Combined	Units
Geometric constant K	4	4.7407	-	-
Filling coefficient ($\phi_{n\rightarrow ne}$)	$0.3682 \rightarrow 0.2447$	$0.3388 \rightarrow 0.2223$	0.2823	-
Axial velocity at exit	5.17	6.29	6.07	m/s
Tangential port velocity	5.06	6.63	-	m/s
Mass-avg tangential velocity	5.4	7.03	6.3	m/s
Mass-avg radius at exit	0.0037	0.0075	0.0074	m
Mixed density at lip	-	-	757.2	kg/m ³
Single-sheet spray angle	92.51	96.38	-	°
Final spray angle	-	-	92.11	°

3.2 Fuel Element

The fuel element, as the name suggests, is the one that injects and gives tangential momentum to the fuel. It has four small inlets of 1mm in diameter. It will be concentric with the oxidizer element. The part will be machined out of stainless steel. An isometric, front cut and top cut views of the part are shown below.

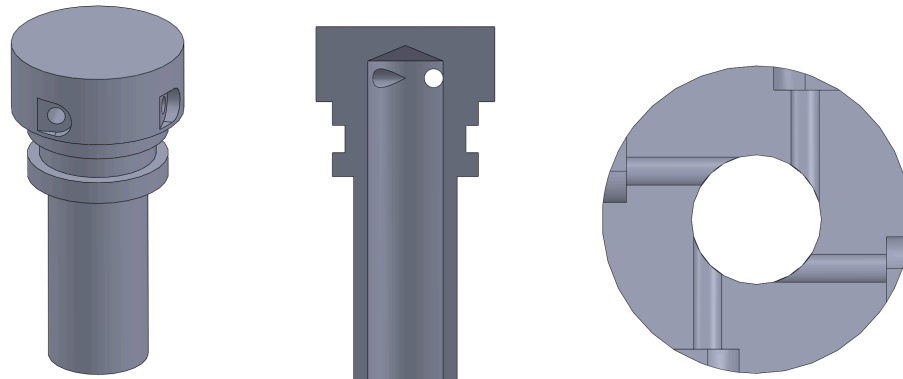


Figure 3. Fuel Element CAD

3.3 Oxidizer Element

Similarly, the oxidizer element injects and gives tangential momentum to the oxidizer. It has six inlets with a diameter of 2mm. It is designed so that the fuel element is recessed in comparison to the oxidizer element. As a consequence, this causes the fuel and oxidizer to mix at the tip before they leave the injector into the combustion chamber. The part will be machined out of stainless steel. An isometric, front cut and top cut views of the part are shown below.

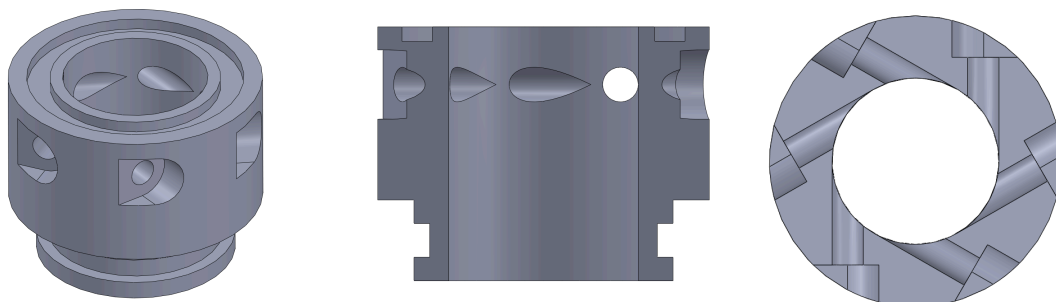


Figure 4. Oxidizer Element CAD

3.4 O-rings

There are only a limited number of compatible materials, both metals and nonmetals, particularly for making gaskets or O-rings. Proper sizing and selection of O-ring material are necessary for proper function of injection elements. An optimal material choice for o-rings are Buna-N (Nitrile rubber) due to its properties for resisting compression and tearing to keep shape over time, additionally there is a wide chemical compatibility along with offering a wide operating temperature range. O-rings grooves were sized using Parker O-Ring Handbook (ORD 5700) specific to sections 4-18 (Static Face Seal Glands).

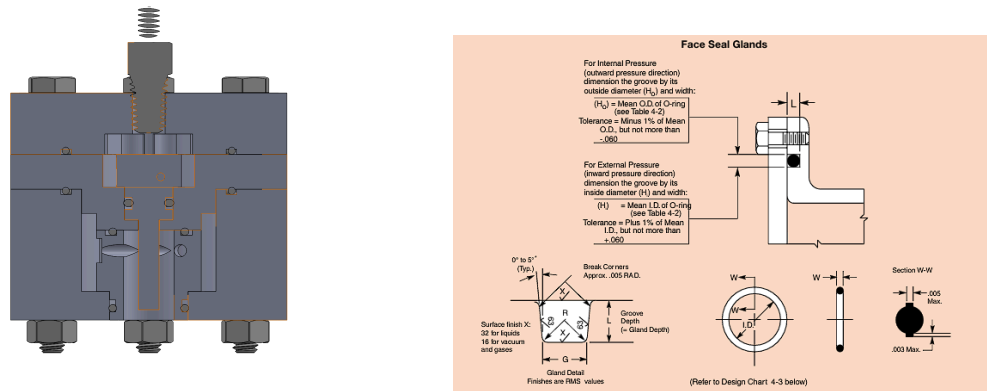


Figure 5. O-rings in Single Element Assembly and Parker Handbook O-ring guide image

Current selection criteria for o-rings consist of 3 sizes to accommodate the single element size and structure to ensure proper sealing, sizes 014, 018, 030 with a durometer rating of 70 (medium hardness). Parameters of squeeze, stretch, and gland fill were all calculated for meeting static sealing guidelines;

$$Squeeze\% = \frac{0.070787 - 0.05}{0.070787} * 100 = 28.651\% ,$$

$$Stretch\% = \frac{0.611023 - 0.739}{0.739} * 100 = - 17.317\% ,$$

$$fill\% = \frac{0.00385}{0.00493} * 100 = 78.1\%$$

After machining of the components, surface roughness plays a critical factor in controlling micro-leaks, macro leaks and uneven squeeze when operating. The finish after CNC operations is sufficient for roughness due to material choice. A roughness average (Ra) of 125 microinches (μ in) or approximately 3.2 micrometers (μ m) will be achieved.

3.5 Flow Simulation

The team has performed several flow simulations to predict spray angle and overall flow interactions. The results are shown below.

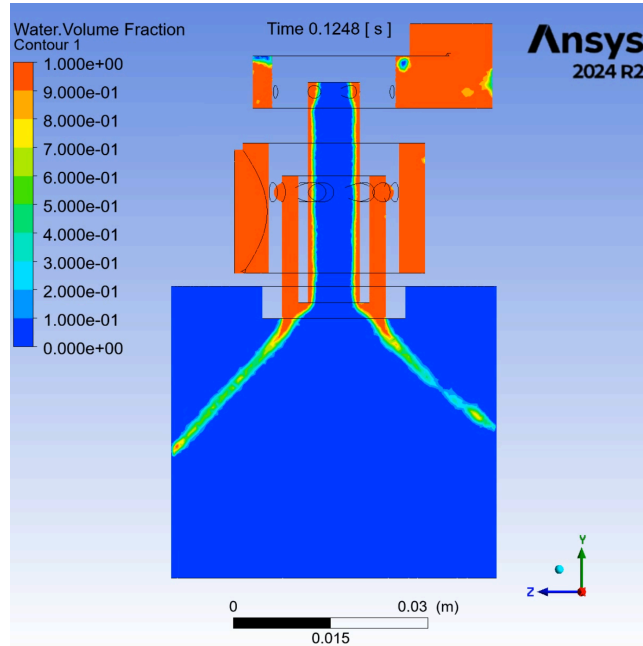


Figure 6. Single Element CFD VOF Simulation

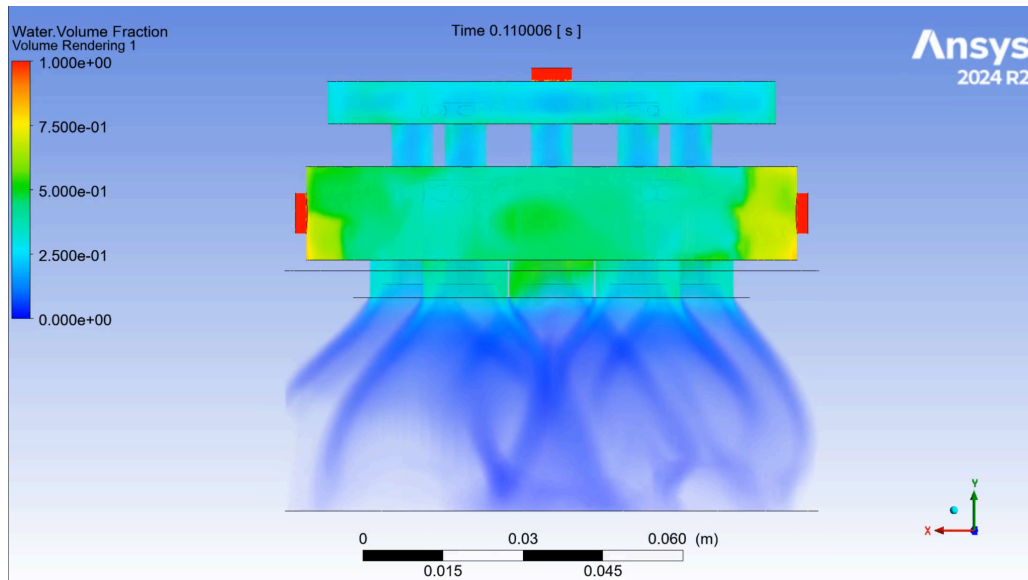


Figure 7. Injector Assembly CFD Mixture Simulation



3.6 Single Element Assembly

In order to test the injector, the team has developed this single element assembly, where the same OF ratio will be provided. The team is expecting to see similar results to the Fluid flow simulations, and to find the discharge coefficient.

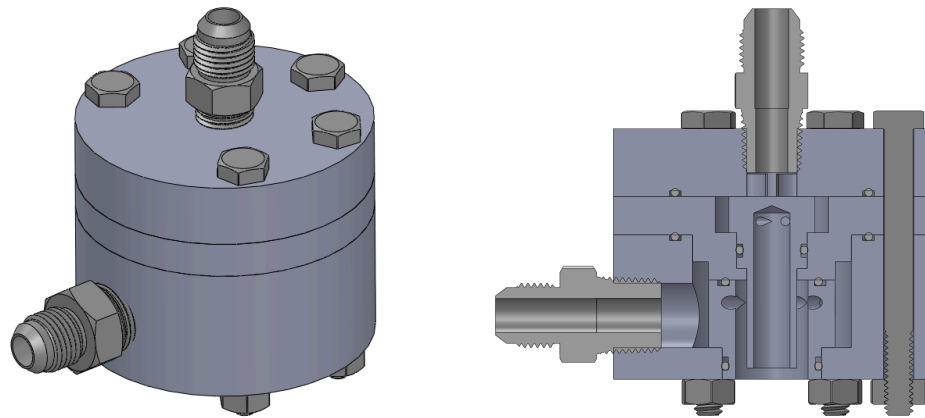


Figure 8. Single Element Assembly

3.7 Georgia Tech Heritage

This injector has been severely influenced by YJSP. The team obtained this information in the first Liquid Propulsion Conference hosted in Georgia Tech. The team is grateful to YJSP for the presentations and important resources given at the conference.



Figure 9. Georgia Tech Single Element water flow test



4 Feed System

The feed system will consist of two 1gal 304 stainless steel propellant tanks pressurized by one main 60 cubic feet nitrogen tank which will feed into the injector element. The figure shown is a proposed layout for piping, instrumentation, and flow control for the system. Components and fittings shall be sourced from McMastercarr and Swagelok due to reliability of materials and supply chain. Key features of the system allow for precise control over what pressure is entering the single element assembly through the use of regulators. Valves will be actuated through the use of high-pressure solenoid valves offering immediate control and effective management of pressure. Key fittings will be AN flared fittings for any flex hoses that may need to be used. Flareless mechanical grip fittings designed to create a leak-tight seal for the fluid system will also be used for main valve lines routing flow throughout. The single element will interface with a 37 degreed AN flared fitting to 1/4 " NPT male for both oxidizer and fuel inlets. A flexible braided chemical hose will be used due to its ability to handle fluids at high pressures up to 3000psi. Sensors such as thermocouples, pressure transducers and venturi flow meters will be used. The oxidizer is typically stored as a saturated liquid to achieve a high storage density while maintaining a moderate tank pressure when kept at low temperatures. As the temperature increases, the liquid partially vaporizes, forming a liquid-vapor mixture due to rising vapor pressure. At sufficiently high temperatures, however, the oxidizer can undergo thermal decomposition, producing gaseous products and releasing heat. Relief vents on top of the propellant tanks will be used to off gas those products.

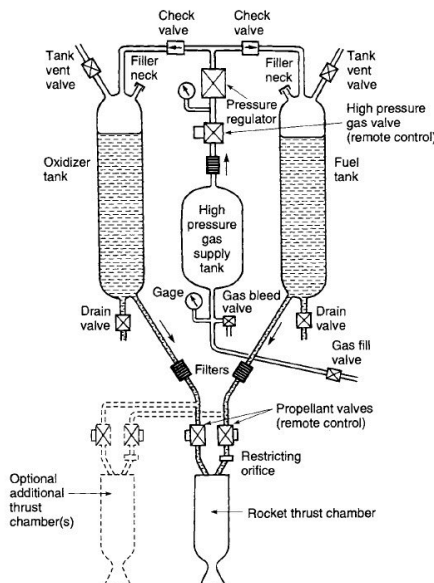


Figure 10. General Pressure Fed Schematic

5 Igniter

The team recognizes the critical importance of the igniter in initiating combustion. However, limited work and analysis have been completed on its design and performance so far. The current plan is to use a nichrome wire as the ignition source, providing sufficient heat to initiate combustion during engine testing.

6 Engine Walls

6.1 Combustion Chamber

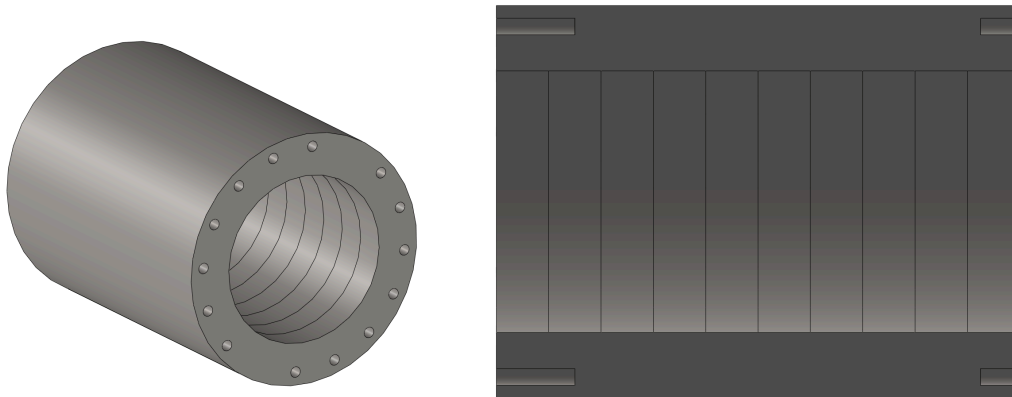


Figure 11. Chamber Wall CAD

Table 7. Combustion Chamber dimensions

Parameter	Value	units
Dc	100	mm
Dt	50	mm
Lcyl	204.12	mm
Lc	277.44	mm
L*	1000	mm
R1	37.5	mm
R2	74.55	mm
b	30	deg

6.2 Nozzle

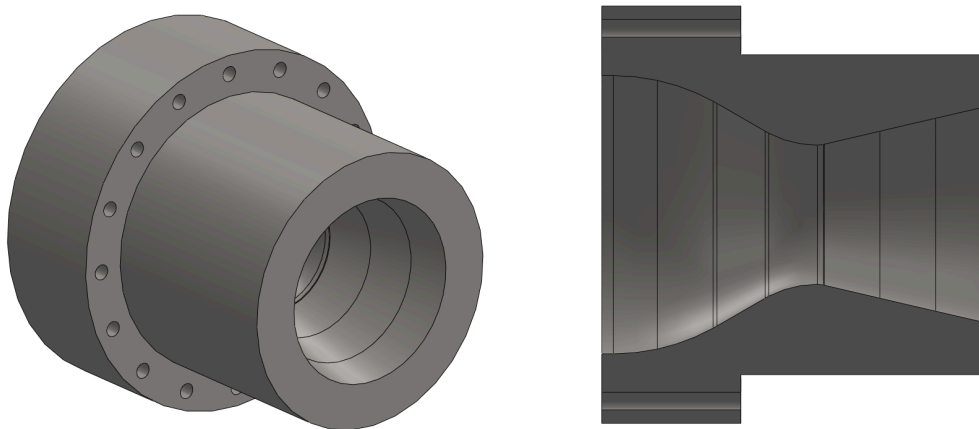


Figure 12. Nozzle CAD

Table 8. Nozzle dimensions

Parameter	Value	units
Type	Parabolic nozzle	-
Rn	9.55	mm
Tn	12.45	deg
Te	21.42	deg
De	74.68	mm
Le	57.47	mm
Le/Dt	1.15	(unitless)
Le/Lc15	121.46	%
Ae/At	2.23	(unitless)

7 Burn time and Cooling Methods

The team realized that one of the limiting factors of the burn time duration would be the melting of the engine walls. Therefore, the team has done a thermal analysis to estimate how long would last before failure.

The team first obtained heat flux values from RPA at different engine walls temperatures. In order to obtain a conservative measurement, the team assumed the maximum heat flux to be constant through the entire burn time. The Heat flux dataset is shown below.

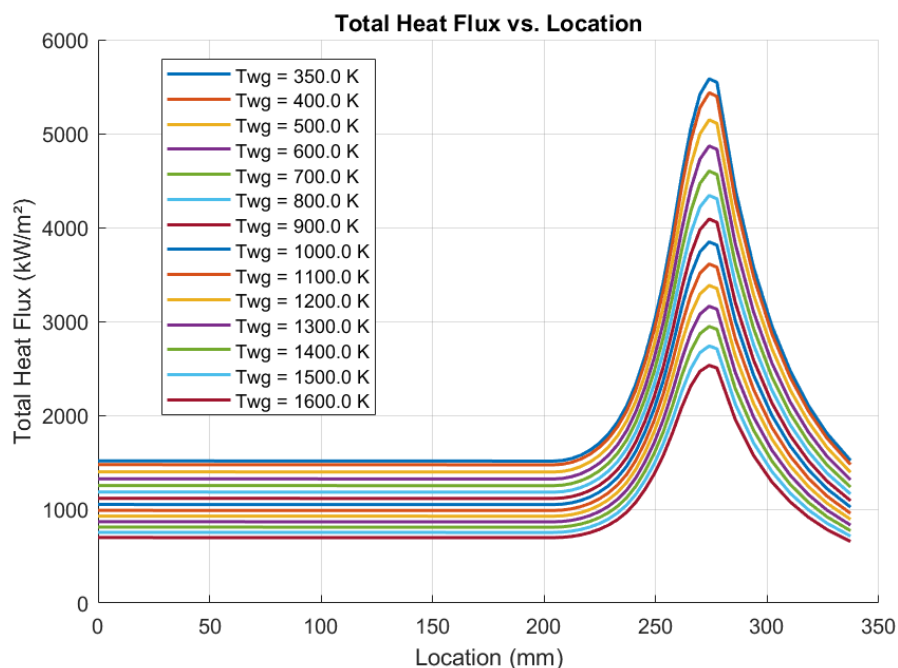


Figure 13. Heat Flux along the engine at different wall temperatures

The team imported this information into SolidWorks to perform a thermal transient study. The simulation was set to last 10 seconds and start at room temperature. The simulation is shown below.



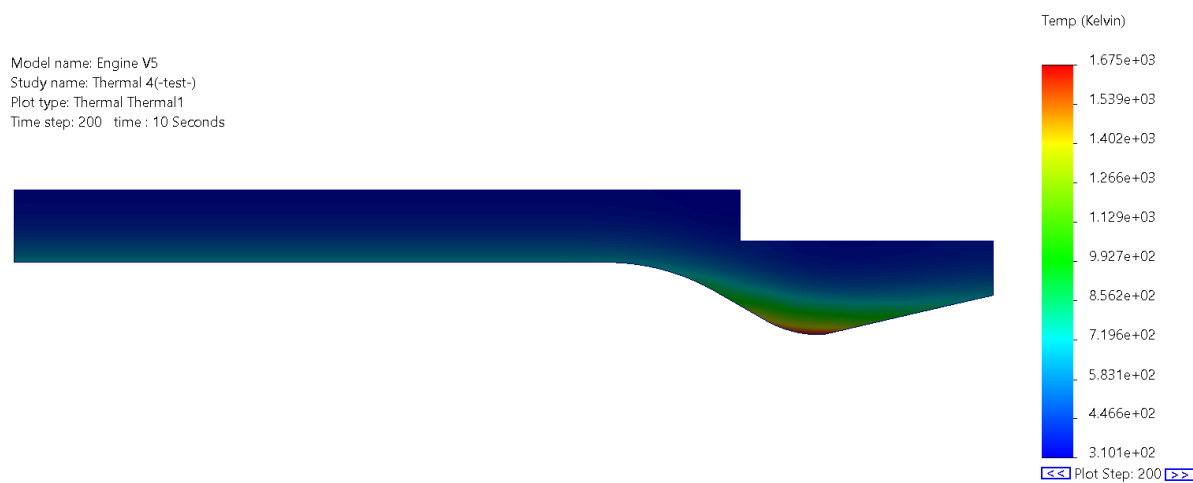


Figure 14. SolidWorks Thermal FEA at 10 seconds

The team set an arbitrary thermal limit of 600 K to the chamber walls. Two nodes were chosen along the engine: one at the chamber walls, and one at the nozzle throat. Given that the node at the throat reached 600 K very quickly, the test would be stopped once the chamber wall node reaches 600 K. This turned out to be at 6 seconds. Results are shown below.

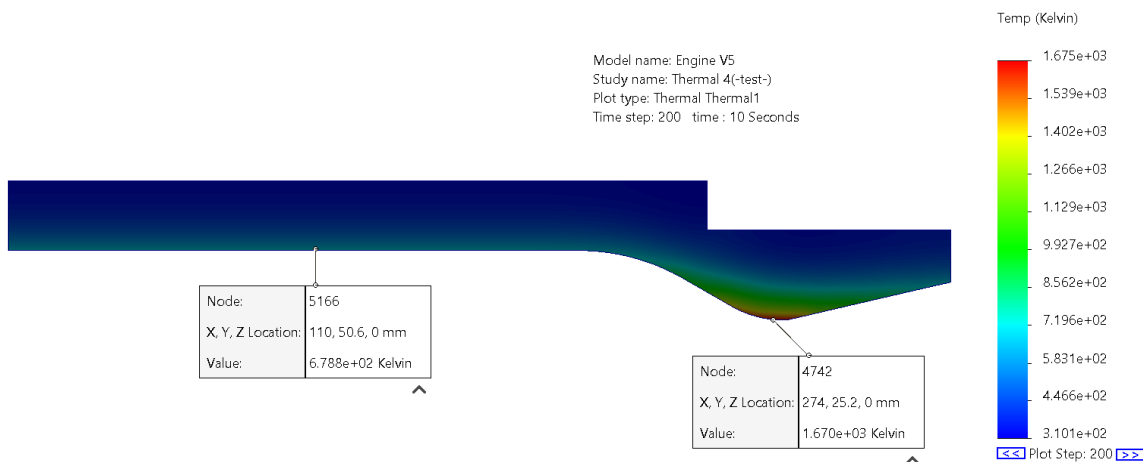


Figure 15. SolidWorks Thermal FEA chamber and nozzle nodes

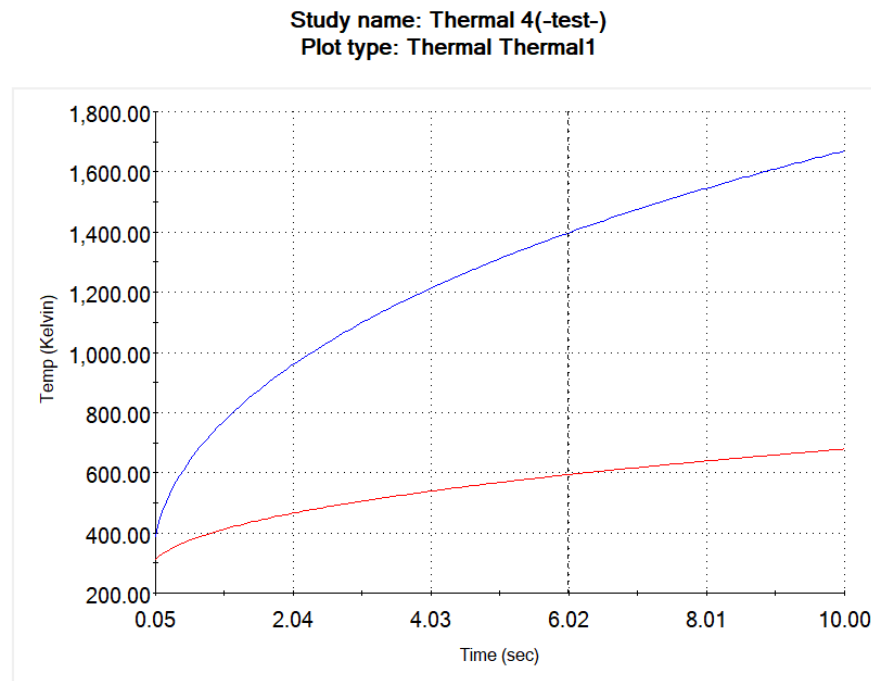


Figure 16. Temperatures over time of chosen nodes

8 Test stand Integration

The engine will be integrated into the Iron Bull test stand. Since the test stand is still under development, the team will wait to determine the appropriate approach for integrating the engine once the design is finalized.

9 Manufacturing

Most, if not all, of the engine manufacturing will be done by third party companies. The team has explored different options, and have decided to proceed with JLC CNC, which charges a total of \$183.52 for 5 parts. A total of two turning operations will be needed for all components. Aluminum 6061 with a tolerance of ± 0.05 in is ideal for reducing costs and lead times for procuring components. Additionally sourcing it from one third party will keep consistency among the entire assembly.